3D Reconstruction Algorithm for Cone-beam Differential Phase Contrast Computed Tomography

Li Zhang, Qiaoguang Fang and Zhifeng Huang

Abstract–**Differential phase contrast computed tomography (DPC-CT) is a novel x-ray inspection method. It reconstructs the refraction index decrement rather than the attenuation coefficient, and can subsequently be applied to inspect weakly absorbing samples. Recently, DPC-CT is implemented, using conventional x-ray tube instead of synchrotron radiation source. In this paper, the reconstruction problem for cone-beam DPC-CT was studied. Some mathematical assumptions were made and a FDK-type algorithm was applied to reconstruct the refractive index decrement distribution of the samples directly from phase contrast projection images. Despite the approximation of our algorithm, it has great features for simplicity of computation and for relatively small errors. The efficacy and shortcoming of the algorithm is presented by its application to a mathematical phantom.**

I. Introduction

In the last decade, supported by the third generation synchrotron radiation source, hard x-ray phase contrast imaging methods have developed rapidly. Phase contrast imaging would play an important role as a nondestructive evaluation and diagnostic technique in medicine, biology, material science and etc. Recent imaging experiments, such as interferometric method[1], in-line method[2], diffraction enhanced imaging (DEI)[3,4], grating-based methods[5-7] show excellent results and exhibit additional advantages, promising to produce images with higher contrast features in the samples, especially weakly absorbing materials.

All of these phase-contrast x-ray imaging technique have been combined with x-ray computed tomography (CT). Momose demonstrated a CT algorithm for interferometric method[8] and implemented it to observe biological specimens and organic materials[9]. Cloetens applied in-line holography to CT for observation of microstructure and damage in materials[10]. Bronnikov presented a linear closed-form solution to the three-dimensional reconstruction problem for in-line holography[11]. Anastasio et al proposed an algorithm to solve the local tomography reconstruction problem for in-line holography[12]. Dilmanian obtained tomographic images of x-ray refraction index using the DEI method[13]. In 2004, Momose et al implemented phase tomography by a phase grating and an amplitude grating in Spring-8[14]. In 2006, Pfeiffer et al firstly retrieved the local gradients of the phase shift distribution by use of three gratings with a conventional x-ray tube according to Talbot Effect and Moiré Interferometry[15] and obtained tomographic phase contrast images in the same experiment platform in the second year[16].

The reconstruction problem for the DEI method and the grating-based method is similar. Refraction-angle images can be retrieved by quantitative extraction methods[4,6,17], which represent the gradients of the refractive index decrement in the sample. These differential phase contrast imaging methods obtain line integral of directional derivatives of refractive index decrements (δ), which is named "directional-derivative projections"[18], and the reconstruction problem for differential phase contrast Computed tomography (DPC-CT) is how to retrieve the primitive function from "directional-derivative projections".

To solve this problem, for parallel-beam, Pavlov et al[19] proposed an indirect algorithm: firstly restore the "directional-derivative projections" to the line integral of δ, and then reconstruct the cross-sectional image of δ by the conventional FBP (filtered backprojection) or CBP (convolution backprojection) algorithm. Zhu et al advised to reconstruct $\nabla\delta$ directly[20]. Maksimenko et al[21] presented another indirect algorithm: firstly reconstruct $\nabla\delta$ and restore δ using an integrating method. Huang et al presented a direct algorithm to solve the reconstruction problem in the parallel-beam case[18]. For fan-beam, Qi et al presented a direct algorithm[22] and solved the local tomography problem via filtered backprojection[23].

Since DPC-CT can be realized with cone-beam X-rays generated by conventional X-ray tube, parallel-beam formula applied to 3D reconstruction of DPC-CT might result in severe artifacts, especially in the case of large objects or short source-to-detector distance. To improve image quality, Feldkamp, Davis and Kress introduced an cone-beam algorithm which is derived from the fan-beam formula, to reconstruct the three-dimensional density function from two-dimensional projections measured in a circular orbit in 1984[24]. Although the algorithm of FDK is approximate, it has great properties, including relatively small errors and simplicity of computation. Subsequently, it has been widely used in the conventional CT and rapidly developed to many derived types considering arbitrary orbits, reconstruction speed and precision. In this paper, we describe a 3D image reconstruction algorithm based on the idea of standard FDK to reconstruct 3D refractive index decrement tomographic image for cone-beam DPC-CT.

Manuscript received November 13, 2008. This work was supported by a grant from the National Natural Science Foundation of China (No. 10875066 and 30770618).

The authors are all with Department of Engineering Physics, Tsinghua University and Key Laboratory of Particle & Radiation Imaging (Tsinghua University), Ministry of Education, Beijing, 100084, China (e-mail: zli@mail.tsinghua.edu.cn, huangzhifeng@mail.tsinghua.edu.cn).

This paper is constructed as follows: in Section 2, parallel-beam and fan-beam reconstruction formulas for DPC-CT are reviewed briefly. In Section 3, the FDK-type algorithm of cone-beam DPC-CT is presented detailedly. In section 4, computer simulation experiments are performed with a mathematical phantom to prove the new algorithm.

II. Reconstruction Formulae for Parallel-beam and Fan-beam DPC-CT

As explained by Davis et al[3] and Keyrilainen et al[25], the angle of X-ray propagation relative to the initial propagation direction is

$$\Theta(t,\theta)\approx\frac{1}{k}\frac{\partial\varphi}{\partial l'}=\int_{l:x\cos\theta+y\sin\theta=t}\frac{\partial\delta}{\partial l'}dl \qquad (1)$$

where k is wave number, φ is phase shift of x-ray propagating across the objects, δ is the refractive index decrement of the objects, l is the path of X-ray beam in the medium and l' is the vertical direction to l. Namely, the angular change is equal to the line integration of directional derivatives of the refractive index decrement. Here the measured data are labeled by the distance t and the angle θ, which specify the direction of the incident x-ray. For example, Fig. 1 shows the refraction angle projection $\Theta(t, \theta)$ of a parallel beam propagating across a cirque-shape phase object.

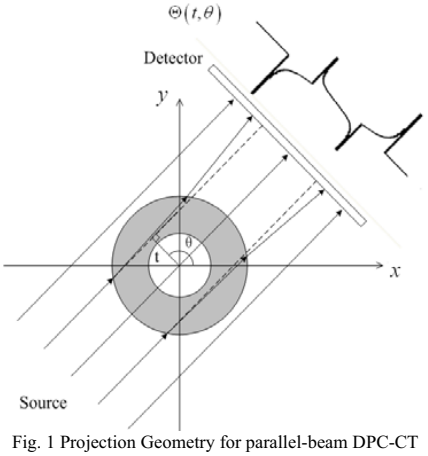

Fig. 1 Projection Geometry for parallel-beam DPC-CT

Huang et al derived a simple formula to solve the parallel-beam reconstruction problem by using Hilbert Filtering[17,18], which could be written as below:

$$\delta(x,y)=\frac{1}{4\pi}\int_0^{2\pi}\int_{-\infty}^{\infty}\Theta_\theta(\omega)\left[-j\,\mathrm{sgn}(\omega)\right]e^{j2\pi\omega t}d\omega d\theta \qquad (2)$$

where $\tilde{\Theta}_\theta(\omega)$ is the Fourier Transformation of $\Theta(\theta, t)$ and

$$\mathrm{sgn}(\omega)=\begin{cases}1 & \omega>0\\ -1 & \omega<0\end{cases}$$

By the convolution theorem, the formula above can be rewritten as:

$$\delta(x,y)=\frac{1}{4\pi^2}\int_0^{2\pi}\int_{-\infty}^{\infty}\Theta(\theta,t)\frac{1}{t'-t}dtd\theta \qquad (3)$$

where t denotes the distance along the straight line corresponding to the detector and t' is a value of t for the ray passing through the point (x, y) under consideration.

In the case of fan-beam scan mode, the acquired data $\Theta(\theta, t)$ have to be relabeled in terms of the angular position Φ of the central ray and the projection position s shown as Fig. 2.

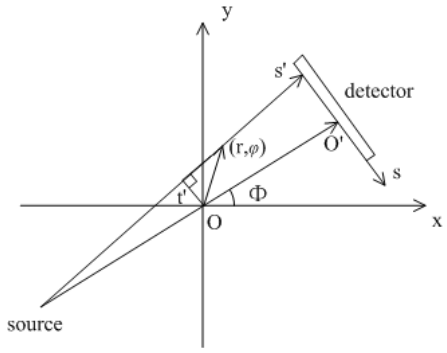

Fig. 2. Projection Geometry for fan-beam DPC-CT

Considering the reconstruction point (r, φ), the fan-beam formula is rewritten in the polar coordinate system[22] as follows:

$$\delta(r,\varphi)=\frac{1}{4\pi^2}\int_0^{2\pi}\frac{1}{U}\int_{-s_m}^{s_m}\Theta(\Phi,s)\frac{1}{s'-s}\frac{RD^2}{D^2+s^2}d\Phi ds \qquad (4)$$

where

$$U=R+r\cos(\Phi-\varphi)$$
$$s'=-\frac{Dr\sin(\Phi-\varphi)}{U} \qquad (5)$$

where R is the distance of the source point from the coordinate origin and D from the detector plane.

Therefore, after the refraction-angle datum $\Theta(\Phi, s)$ are retrieved and modified with a geometrical factor $RD^2/(D^2+s^2)$, a convolution step can be performed to generate the filtered data. Finally, a reconstructed image of δ can be obtained after weighted back-projection.

III. A FDK-type Reconstruction Formula for Cone-beam DPC-CT

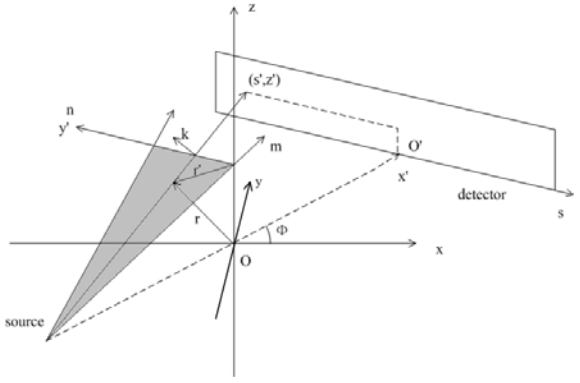

Fig. 3. Projection Geometry for cone-beam DPC-CT

Using the coordinate system shown in Fig. 3, the reconstruction formula for fan-beam case can be rewritten in vector form as follows:

$$\delta(\vec{r}) = \frac{1}{4\pi^2}\int \frac{1}{R+\vec{r}\cdot\hat{m}} d\Phi \int_{-\infty}^{\infty} \Theta_{\Phi}(s) \frac{1}{s'-s} \frac{RD^2}{D^2+s^2} ds \quad (6)$$

where

$$s' = \frac{D\vec{r}\cdot\hat{n}}{R+\vec{r}\cdot\hat{m}} \quad (7)$$

All X-rays from some angle Φ of the source that pass through the detector plane along a line Z=const form a fan-shape section. If Z=0, this section is as same as the case of fan-beam scan mode and we can use Eq. (5) to reconstruct the exact values of refractive index decrement in the mid-plane. If *Z=const*≠0, this section is tilted and some correction should be performed for this formula. First, the equivalent rotation d*Φ*' about the normal to the section must be corrected with:

$$d\Phi' = d\Phi \frac{R}{\sqrt{R^2+Z^2}} \quad (8)$$

where d*Φ* is the actual rotation about the vertical axis and *R* is the source-to-origin distance. Further, the source-to-origin distance *R*' and the source-to-detector distance *D*' in the tilted fan-shape plane are different from those in the mid-plane, whose relationships can be written as follows:

$$R' = \sqrt{R^2+Z^2}$$
$$D' = \frac{R'}{R} D \quad (9)$$

Any reconstruction point can be written as $\vec{r} = \vec{r}' + Z\hat{z}$, then each value of refractive index decrement can be calculated in the form of the fan-beam reconstruction formula:

$$\delta(\vec{r}) = \delta(\vec{r}' + Z\hat{z}) \approx \frac{1}{4\pi^2}\int \frac{1}{R'+\vec{r}'\cdot\hat{m}} d\Phi' \int_{-\infty}^{\infty} \Theta_{\phi}(s,Z) \frac{1}{s'-s} \frac{R'D'^2}{D'^2+s^2} ds \quad (10)$$

where

$$s' = \frac{D'\vec{r}'\cdot\hat{n}}{R'+\vec{r}'\cdot\hat{m}}$$
$$Z = \frac{D\vec{r}\cdot\hat{z}}{R+\vec{r}\cdot\hat{x}'} \quad (11)$$

Substitute Eq. (10) with Eq. (8) and Eq. (9), we have

$$\delta(\vec{r}' + Z\hat{z}) = \frac{1}{4\pi^2}\int \frac{1}{R+\vec{r}\cdot\hat{x}'} d\Phi \int_{-\infty}^{\infty} \Theta_{\Phi}(s,Z) \frac{1}{s'-s} \frac{D^2\sqrt{R^2+Z^2}}{D^2\left(1+Z^2/R^2\right)+s^2} ds \quad (12)$$

where

$$s' = \frac{D\vec{r}\cdot\hat{y}'}{R+\vec{r}\cdot\hat{x}'}$$
$$Z = \frac{D\vec{r}\cdot\hat{z}}{R+\vec{r}\cdot\hat{x}'} \quad (13)$$

Here we have used two relationships: $\vec{r}'\cdot\hat{m} = \frac{R'}{R}\vec{r}\cdot\hat{x}'$ and $\vec{r}'\cdot\hat{n} = \vec{r}\cdot\hat{y}'$.

Similar to the fan-beam case, this FDK-type reconstruction formula for cone-beam DPC-CT can be performed in 3 steps:

First, pre-weight the acquired refraction data point by point with the factor of $\frac{D^2\sqrt{R^2+Z^2}}{D^2\left(1+Z^2/R^2\right)+s^2}$.

Second, a series of one-dimensional convolutions are carried out to filter the pre-weighted refraction data with Hilbert filtering kernel of 1/*s*.

Finally, back-project the filtered data with the factor of $1/(R'+\vec{r}\cdot\hat{x}')$ for each reconstruction point. Three dimensional distribution of δ is obtained.

The DPC-CT cone-beam reconstruction formula is different from standard FDK formula for absorption CT in three aspects: the pre-weighting function, the filtering kernel in the filtering step and the distance weighting function in backprojection step.

IV. Computer Simulation Experiments

In order to validate the efficacy of our algorithm, we apply it to a mathematical phantom described in Table 1. The phantom is designed by superposing the contributions of δ of eight ellipsoids. The first two generate an inner cylinder and an outer cylindrical shell. This phantom is similar with that given by Feldkamp et al[24], but it is constructed by refractive index decrement, the attenuation coefficient distribution of which is assumed to be zero. As explained by Feldkamp, this particular phantom embodies potential difficulties, such as abrupt edge, asymmetrically placed objects and slight differing of refractive index decrement of the samples. Refraction-angle data were formed from the phantom as analytically derived "directional derivative projections", which has been shown in Eq. 1. The distance between the x-ray source and rotational axis is assumed to be 15mm, and the detector plane is set 25mm apart from source. The cone angle of the divergent beam is large enough to cover all the ellipsoids. The angular position is sampled from 0° to 360°, with a sampling rate of 1°. The detector matrix contains 256×256 units, whose pixel size is 0.1mm×0.1mm. To encompass the objects of interest, the reconstruction mesh extends 10.24mm by 10.24mm horizontally and 4mm vertically, containing 256 × 256 × 100 points. For display, we have chosen five horizontal planes, equally spaced and symmetrically located above or below the mid-plane.

Table I
Phantom Details

OBJ	Position /mm			Radii /mm			δ
	x	y	z	x	y	z	
1	0	0	0	4	4	∞	3.5×10^{-6}
2	0	0	0	3.5	3.5	∞	-2×10^{-6}
3	0	0	0	3	2	2	5×10^{-7}
4	-0.5	0	0.5	1.1	1.1	1.1	9×10^{-8}
5	-0.7	-0.6	-0.5	1.4	1.6	1.1	7×10^{-7}
6	0.8	0.8	0.2	1.2	0.8	1.6	2×10^{-7}
7	-1.3	0	0.8	0.9	0.9	0.3	5×10^{-7}
8	0.4	-1.2	0.8	0.9	0.9	0.3	5×10^{-7}

The exact digitized representation of the phantom and the reconstruction results of the selected sections reconstructed by our algorithm are shown in Fig. 4 for comparison. According to the result, the distribution of δ generated by our algorithm is close to the exact values. Although it is difficult to observe the low-contrast features in the gray scale used here, the difference of δ is clear in the plot of a single selected line. As expected, band limiting results in rounding of abrupt edge. Fig. 5 shows the volume rendering result of the phantom calculated by VTK toolkits. The vertical strip artifacts on the cylinder

walls are caused by the limit projections and other approximations. The 4th ellipsoid is difficult to recognize, because the gray scale used here cannot show its slight differing from the surroundings. Despite of these shortcomings, our algorithm is faithful.

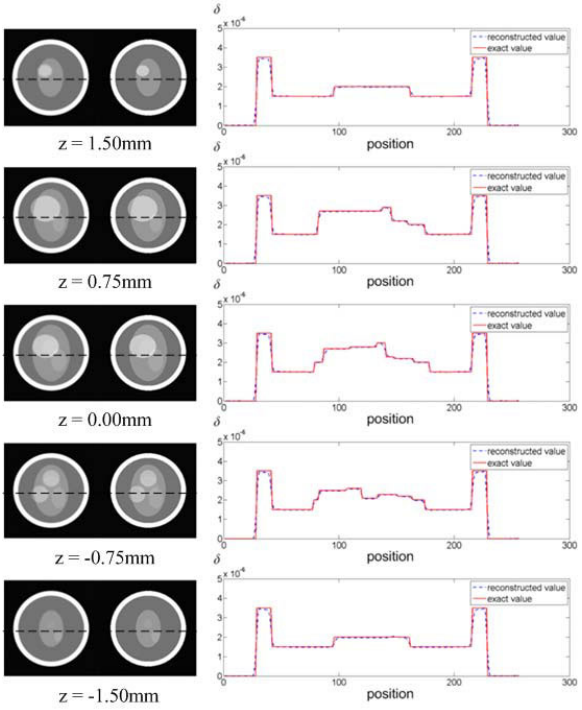

Fig. 4. Comparison of representative slices of the phantom with its reconstruction. The left row of slices is the reconstruction results of the phantom, with the corresponding exact digitized representations on the right. The values along the central horizontal line of each slices has been plotted, comparing the refractive index decrements of the phantom (solid line) with that of the reconstruction (dashed line).

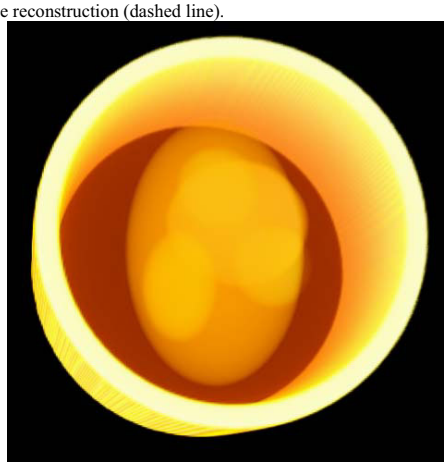

Fig. 5. Volume rendering result of the phantom

Although some correction steps have been carried out, the reconstruction errors might be expected in the plane far from the mid-plane. In Fig. 6, we display and compare vertical plane x=0 of the phantom with the results reconstructed by our algorithm. The values of δ in the axis z are also plotted. Clearly, the values of δ are smaller in other planes than in the mid-plane. Further the plane is from the mid-plane, greater the errors are. This phenomenon is as same as that in absorption-CT. Many correction algorithms have been presented, which might be adapted for DPC-CT.

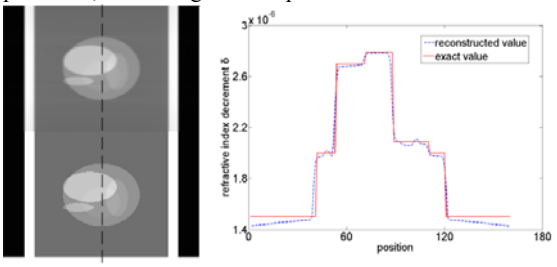

Fig. 6. Comparison of vertical plane (x=0) of the exact phantom (the lower row) with corresponding plane reconstructed by our algorithm (the upper row). The vertical line defines the position corresponding to the line drawing in the right hand side, in which δ of the phantom (solid line) is compared with that of the reconstruction (dashed line).

V. CONCULUSION

In this paper, we derived and validated a FDK-type reconstruction formula for cone-beam DPC-CT. Although this algorithm is approximate except the mid-plane, the errors are relatively small and it is easy to implement. It works well for a mathematical phantom. More correction steps should be developed for the planes far from the mid-plane, and it can be adapted for general trajectory.

ACKNOWLEDGMENT

We appreciate Prof. Yu-Xiang Xing and Dr. Liang Li for their fruitful discussions.

REFERENCES

[1] Momose A, Takeda T, Itai Y and Hirano K, "Phase-contrast X-ray computed tomography for observing biological soft tissues," *Nature Medicine*, vol. 2, pp. 473-475, 1996

[2] Snigirev A, Snigireva I, Kohn V, Kuznetsov S and Schelokov I, "On the possibilities of x-ray phase contrast microimaging by coherent high-energy synchrotron radiation," *Rev. Sci. Instrum.*vol. 66, pp. 5486-5492, 1995

[3] Daivs T J, Gao D, Gureyev T E, Stevenson A W and Wilkins S W, "Phase-contrast imaging of weakly absorbing materials using hard X-rays," *Nature,* vol. 373, pp. 595-597, 1995

[4] Chapman D, Thomlinson W, Johnston R E, Washburn D, Pisano E, Gmür N, Zhong Z, Menk R, Arfelli F and Sayers D, "Diffraction enhanced x-ray imaging," *Phys. Med. Biol.,* vol. 42, pp. 2015-2025, 1997

[5] Momose A, Kawamoto S, Koyama I and Suzuki Y, "Phase tomography using an X-ray talbot interferometer," *Proc. of SPIE,* vol 5535, pp. 352-360, 2004

[6] Weitkamp T, Diaz A, David C, Pfeiffer F, Stampanoni M, Cloetens P and Ziegler E, "X-ray phase imaging with a grating interferometer," *Opt. Express,* vol. 13, pp. 6296-6304, 2005

[7] Engelhardt M, Baumann J, Schuster M, Kottle C, Pferffer F and Bunk O, "High-resolution differential phase contrast imaging using a magnifying projection geometry with a microfocus x-ray source," *Appl. Phys. Lett.,* vol. 90, pp. 224101, 2007

[8] Momose A, "Demonstration of phase-contrasat X-ray computed tomography using an X-ray interferometer," *Nuclear Instruments and Methods in Physics Research,* vol. A352, pp. 622-628, 1995

[9] Momose A, Takeda T and Itai Y, "Phase-contrast x-ray computed tomography for observing biological specimens and organic materials," *Rev. Sci. Instrum.,* vol. 66, pp. 1434-1436, 1995

[10] Cloetens P, Pateyron-Salomé M, Buffière J Y, Peix G, Baruchel J, Peyrin F and Schlenker M, "Observation of microstructure and damage in materials by phase sensitive radiography and tomography," *J. Appl. Phys*., vol. 81, no. 9, pp. 1, 1997

[11] Bronnikov A V, "Reconstruction formulas in phase-contrast tomography," *Optics Communications,* vol. 171, pp. 239-244, 1999

[12] Anastasio M A, Carlo F D and Pan X C, "Phase-contrast tomography and the local tomography problem," *Proc. Of SPIE,* vol. 5030, pp. 120-126, 2003

[13] Dilmaniant F A, Zhong Z, Ren B, Wu X Y, Chapman L D, Orion I and Thomlinson W C, "Computed tomography of x-ray index of refraction using the diffraction enhanced imaging method," *Phys. Med. Biol.,* vol. 45, pp. 933-946, 2000

[14] Momose A, Kawamoto S, Koyama I and Suzuki Y, "Phase tomography using an X-ray talbot interferometer," *Proc. Of SPIE,* vol. 5535, pp. 352-360, 2004

[15] Pfeiffer F, Weitkamp T, Bunk O and David C, "Phase retrieval and differential phase-contrast imaging with low-brilliance X-ray sources," *Nature physics,* vol. 2, pp. 258-261, 2006

[16] Pfeiffer F, Kottler C, Bunk O and David C, "Hard X-ray phase tomography with low-brilliance sources," *Phys.Rev.Lett*., vol. 98, pp. 108105, 2007

[17] Huang Z F, Kang K J, Zhu P P, Huang W X, Yuan Q X and Wang J Y, "Strategy of extraction methods and reconstruction algorithms in computed tomography of diffraction enhanced imaging," *Phys. Med. Biol.,* vol. 52, pp. 1-12, 2007

[18] Huang Z F, Kang K J, Li Z, Zhu P P, Yuan Q X, Huang W X, Wang J Y, Zhang D and Yu A M, "Direct computed tomographyic reconstruction for directional-derivate projections of computed tomography of diffraction enhanced imaging," *Appl. Phys. Lett.,* vol. 89, pp. 041124, 2006

[19] Pavlov K M, Kewish C M, Davis J R and Morgan M J, "A variant on the geometrical optics approximation in diffraction enhanced tomography," *J. Phys. D: Appl. Phys*., vol. 34, pp. A168-A172, 2001

[20] Zhu P P, Wang J Y, Yuan Q X, Huang W X, Shu H, Gao B, Hu T D and Wu Z Y, "Computed tomography algorithm based on diffraction-enhanced imaging setup," *Appl. Phys. Lett.,* vol. 87, pp. 264101, 2005

[21] Maksimenko A, Ando M, Hiroshi S and Yuasa T, "Computed tomographic reconstruction based on x-ray refraction contrast," *Appl. Phys. Lett.,* vol. 86, pp. 124105, 2005

[22] Chen G H and Qi Z H, "Image reconstruction for fan-beam differential phase contrast computed tomography," *Phys. Med. Biol.,* vol. 53, pp. 1015-1025, 2008

[23] Qi Z H and Chen G H, "A local region of interest image reconstruction via filtered backprojection for fan-beam differential phase-contrast computed tomography," *Phys. Med. Biol.,* vol. 52, pp. N417–N423, 2007

[24] Feldkamp L A, Davis L C and Kress J W, "Practical cone-beam algorithm," *J. Opt. Soc. Am. A,* vol. 1, pp. 612-619, 1984

[25] Keyrilainen J, Fernandez M and Suortti P, "Refraction contrast in X-ray imaging," *Nuclear Instruments and Methods in Physics Research A,* vol. 488, pp. 419-427, 2002